Journal of
Nanoscience and Nanotechnology
Vol. 9, 1423–1427, 2009

Fabricating Nano Ribbons and Nano Fibers of Semiconductor Materials by Diamond Turning

Jiwang Yan[1,*], Xiaohui Gai[2], and Tsunemoto Kuriyagawa[1]

[1] *Department of Nanomechanics, Tohoku University, Aramaki Aoba 6-6-01, Aoba-ku, Sendai, 980-8579, Japan*
[2] *Department of Metallurgy, Material Science and Material Processing, Tohoku University, Aramaki Aoba 6-6-02, Aoba-ku, Sendai, 980-8579, Japan*

Diamond turning tests have been made on single crystalline silicon wafers. It was found that chips removed from the material surface during machining consist of nano needles, nano ribbons and nano fibers, the shape and size of which depend on the undeformed chip thickness and the cutting edge geometry. Electron diffraction studies showed that the needle-type chips are micro-crystalline with slight amorphization; while the nano ribbons and nano fibers have been mostly transformed into the amorphous phase. This work preliminary demonstrated the feasibility of an efficient and inexpensive production method for mechanically flexible nano ribbons and nano fibers for micro-nano mechanical and electronic applications.

Keywords: Diamond Turning, Ductile Machining, Semiconductor, Silicon, Chip Formation, Nano Ribbon, Nano Fibber, Amorphous, Phase Transformation.

1. INTRODUCTION

Diamond turning is an important machining technology for producing precision optical, optoelectronic and mechanical elements.[1–3] By using numerically controlled ultraprecision machines and extremely sharp diamond cutting tools, components with extremely high accuracy and fine surface finish can be fabricated. As a byproduct of the diamond turning process, extremely small cutting chips will be removed from the workpiece materials during machining. These chips have been usually considered useless and disposed as wastes.

On the other hand, the potential needs for nano fibers, nano needles and nano ribbons of semiconductors are increasing in the nanotechnology era. For example, aligned arrays of submicron ribbons of single-crystal silicon have been recently used in thin-film transistors.[4] Silicon nano wires have been fabricated into field-effect transistors, biological and chemical sensors, light-emitting devices, MEMS cantilever sensors[5–10] and so on. These nano components of semiconductors have been usually fabricated by vapor-liquid-solid growth,[11–13] solution phase synthesis,[14,15] thermal-evaporation oxide-assisted growth,[16,17] and lithography related etching methods.[18]

The purpose of the present work is to investigate the feasibility of fabricating nano fibers and nano ribbons by diamond turning through controlling the microscopic chip formation behavior. Compared to the physical and chemical methods, diamond turning can be carried out in atmosphere at room temperature without the need for strict vacuum conditions or other special environments. The production efficiency can be very high and the production cost is relatively low.

2. EXPERIMENTAL DETAILS

The principle and the machining model of diamond turning are schematically shown in Figures 1(a) and (b), respectively. The workpiece is rotated by a high speed spindle. The cutting tool is subjected to a transverse feed (f) per revolution of the workpiece in x direction at a certain depth of cut in z direction; hence, a large flat surface consisting of extremely fine cutting marks can be produced. In Figure 1(b), undeformed chip thickness h is determined by cutting edge angle κ and tool feed f. Thus, by using a sufficiently small κ and/or a sufficiently small f, it is possible to thin the undeformed chip thickness h to the nanometric range over the entire cutting region.

Diamond turning experiments were carried out on a numerically controlled multi-axis ultraprecision lathe. The lathe has an air-bearing spindle, two perpendicular linear tables and a rotary table. The linear tables are supported by high-stiffness hydrostatic bearings and are driven by servomotors via hydrostatic screws, allowing smooth

*Author to whom correspondence should be addressed.

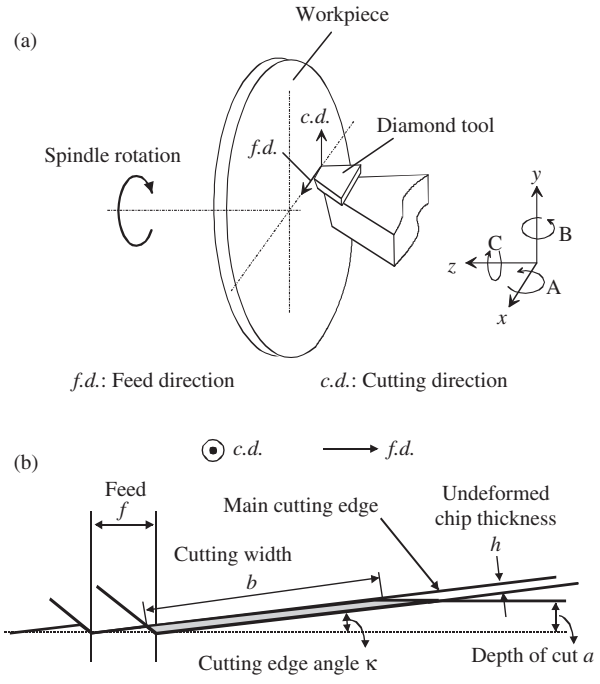

Fig. 1. Schematic presentation of (a) diamond turning and (b) its machining model.

nanometric movement with negligible mechanical friction. The rotary table is also supported by hydrostatic bearings and driven by a friction drive in order to prevent from backlash movements. Laser hologram scales are used to accurately position all these tables. Under precise numerical control, the linear tables can be moved precisely at a resolution of 10 nm per step. To isolate the lathe from environmental vibration, the main section of the machine was mounted onto a granite bed, which is supported by a set of air mounts.

Device grade p-type single-crystal silicon wafers with plane orientation (111) were used as specimens. These wafers are 76.2 mm in diameter, 1.2 mm in thickness and obtained with chemomechanical polished finishes. The workpieces were vacuum-chucked to the machine spindle. A cutting tool made of single crystalline diamond with a $-20°$ rake angle and a $\sim$50 nm edge radius was used. Undeformed chip thickness h was varied from 0 to 500 nm by changing the tool feed f and cutting edge angle κ. The depth of cut (a) was set to 2$\sim$5 μm. The rotation rate of the machine spindle was fixed to 1500 rpm. Consequently, the cutting speed changes from 0 to 5.98 m/s during a facing cut. Dry cutting was performed without any cutting fluid.

3. RESULTS AND DISCUSSION

When diamond turning tests were performed at various undeformed chip thicknesses, dramatic changes in chip formation behavior were confirmed. Figure 2(a) shows an SEM photograph of chips generated at an undeformed chip

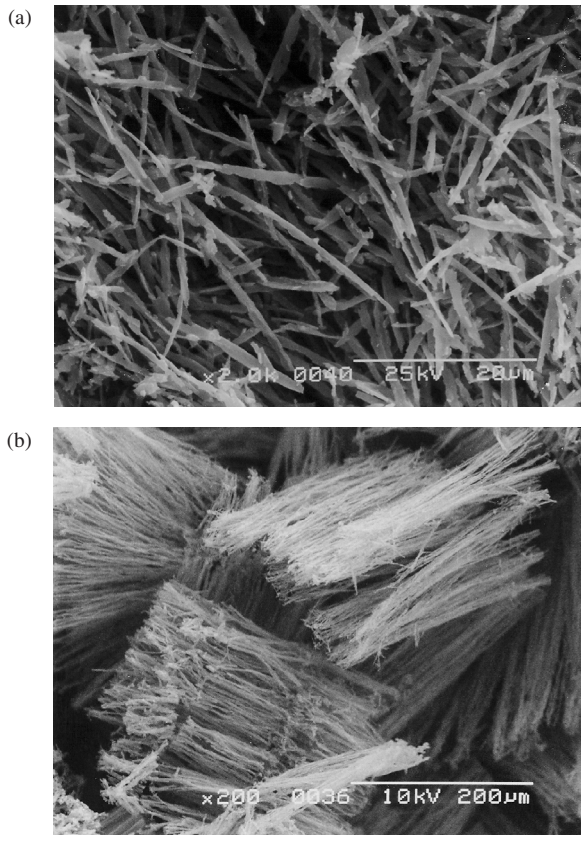

Fig. 2. SEM photographs of needle-type chips of silicon generated at an undeformed chip thickness of (a) 460 nm and (b) 163 nm.

thickness of 460 nm. These chips were formed as spatially disordered micro needles. The thickness of the needles is in the submicron to micron level and the length is a few tens of microns. The average length of the needles is significantly smaller than the cutting width b (in this case $b = 265$ μm), indicating that the needles have been broken along the edge direction. When the undeformed chip thickness was decreased to 163 nm, as shown in Figure 2(b), the needle-shaped chips begin to be piled in good order

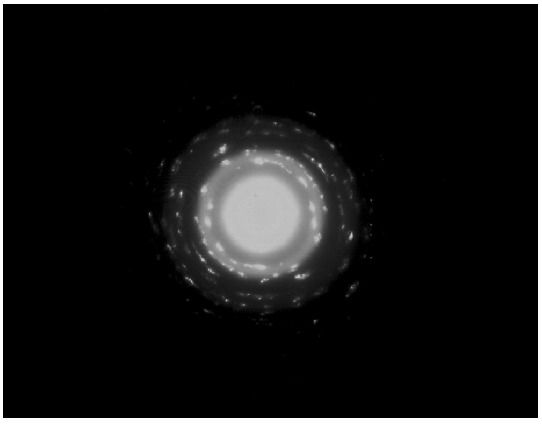

Fig. 3. Electron diffraction pattern of the silicon needles in Figure 2(b), indicating a mixture of micro-crystalline phase and amorphous phase.

Fig. 4. SEM photograph of ribbon-type chips of silicon generated at an undeformed chip thickness of 58 nm.

and their lengths becomes the same as the cutting width b, indicating that the machining mode under this condition is uniform over the entire cutting width. The needle-type chips are geometrically akin to the shear-type chips in traditional hard metal cutting.

To confirm the microstructure of the needle chips, selected area electron diffraction analysis was made. Figure 3 shows the diffraction pattern of the nano needles shown in Figure 2(b). In the figure, irregular diffraction spots are predominant, indicating that the needles are mainly microcrystalline; while halo rings are also shown, demonstrating that amorphization of silicon has also occurred.

As the undeformed chip thickness was further decreased, the chips transited from the needle type to a ribbon type. Figure 4 shows an SEM photograph of chips formed at $h = 58$ nm. The chips are long and continuous ribbons similar to those generated when machining ductile metals such as aluminum and copper. Figure 5 shows the diffraction pattern of the ribbon chips. In the figure, halo rings are clearly shown while the diffraction spots have been seriously deformed and cannot be clearly identified. This fact demonstrates that amorphous silicon is predominant in the ribbon-type chips.

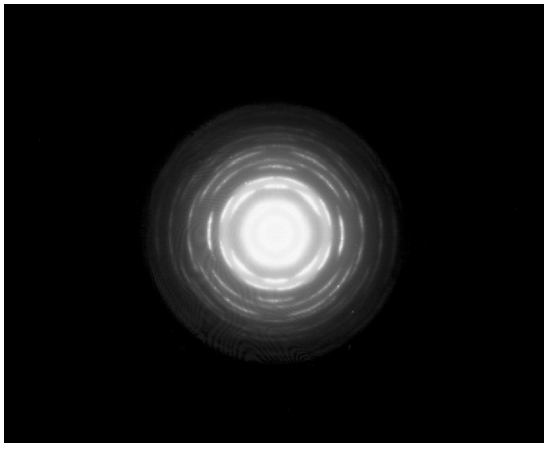

Fig. 5. Electron diffraction pattern of the silicon ribbons in Figure 4, showing an amorphous microstructure.

Figure 6(a) shows an SEM photograph of chips formed at $h = 18$ nm. The chips appear to be very long and uniform ribbons. However, when observing at a higher magnification as shown in Figure 6(b), we found that the ribbon chip has a sponge-like loose structure, distinctly different from the solid ribbons shown in Figure 4. Figure 6(c) is a close-up view of the chip surface. It is seen that the chip

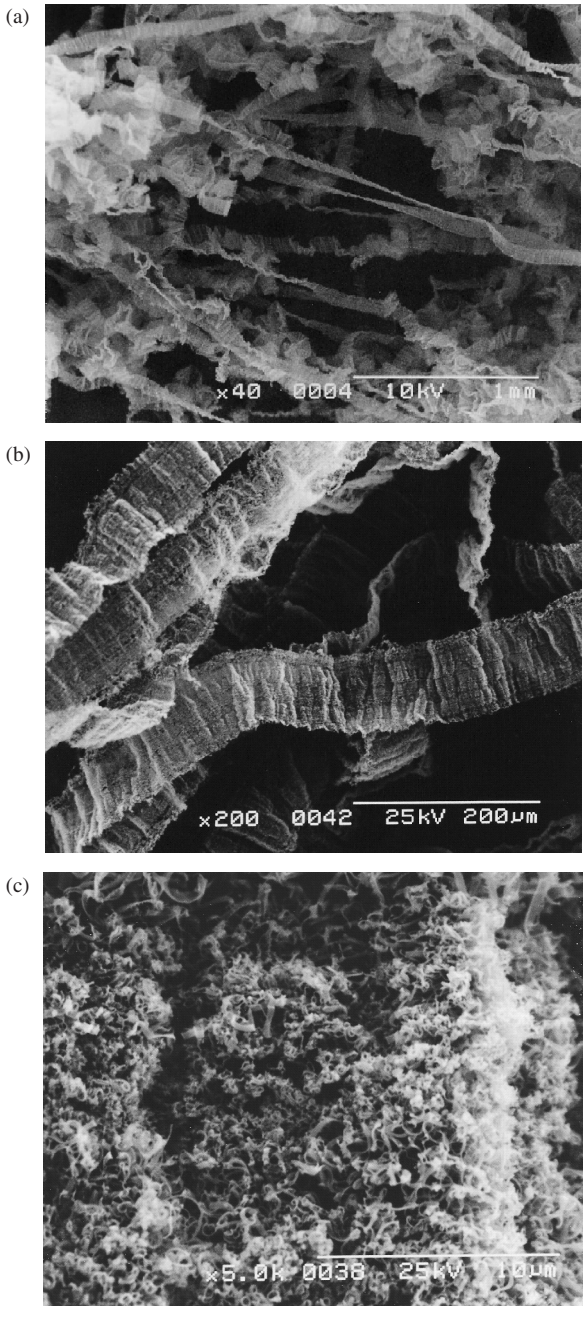

Fig. 6. SEM photographs of fiber-type chips of silicon generated at an undeformed chip thickness of 18 nm. Photos (a∼c) were taken at different magnifications.

consists of numerous fine fibers which curl and interweave. Electron diffraction analysis showed that the fibers were amorphous.

Chip formation behavior was also found to change with the tool edge geometry. Figure 7(a) shows chips generated under the same condition as that of Figure 6 after the cutting edge has been worn. It can be seen that the fine fibers become longer and interweave in a much looser manner than the sponge-like ribbons in Figure 6. Figure 7(b) is a magnified photograph of the fibers. The fibers have submicron level thickness and micron level width. The curvatures of the fibers are also larger than that in Figure 6(c).

Silicon is a nominally brittle material having a strong directional covalent bonding with a diamond structure. At room temperature, the dislocations are immobile and hence single crystalline silicon responds in a brittle manner. However, it has been known that under specific conditions such as high temperature and high pressure, silicon can also be deformed plastically. In diamond turning, by using a sufficiently small undeformed chip thickness, silicon can be machined in a completely ductile mode.[19–21] Ductile machining is considered to be facilitated by the high-pressure phase transformation of silicon from the diamond cubic structure to the metallic and amorphous structures.[22–24]

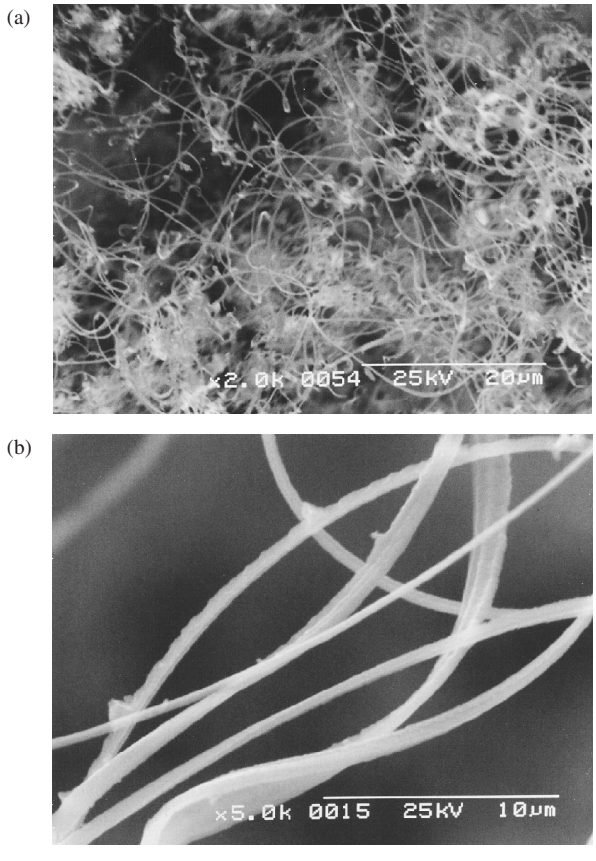

Fig. 7. SEM photographs of fiber-type chips of silicon formed at an undeformed chip thickness of 18 nm using a worn and grooved tool. Photos (a and b) were taken at different magnifications.

Proposed chip formation models are shown in Figure 8. As shown in Figure 8(a), the needle-type chips are considered to be generated in a brittle-ductile transition mode where the machining pressure is not high enough to cause the complete phase transformation of silicon. The machining pressure fluctuates at a high frequency, causing the strain energy in workpiece material to vary periodically. Under this condition, only a portion of removed material will undergo phase transformation due to the high pressure near the tool tip; while most material in other region remains crystalline.

Figure 8(b) shows the ribbon-type chip formation model. When undeformed chip thickness becomes sufficiently small and approaches the same level as the cutting edge radius, the cutting region will be under an extremely high hydrostatic pressure condition which leads to complete phase transformations of silicon. The material ductility will be significantly improved by the phase transformation and the stable material flow will form a uniform continuous ribbon chip.

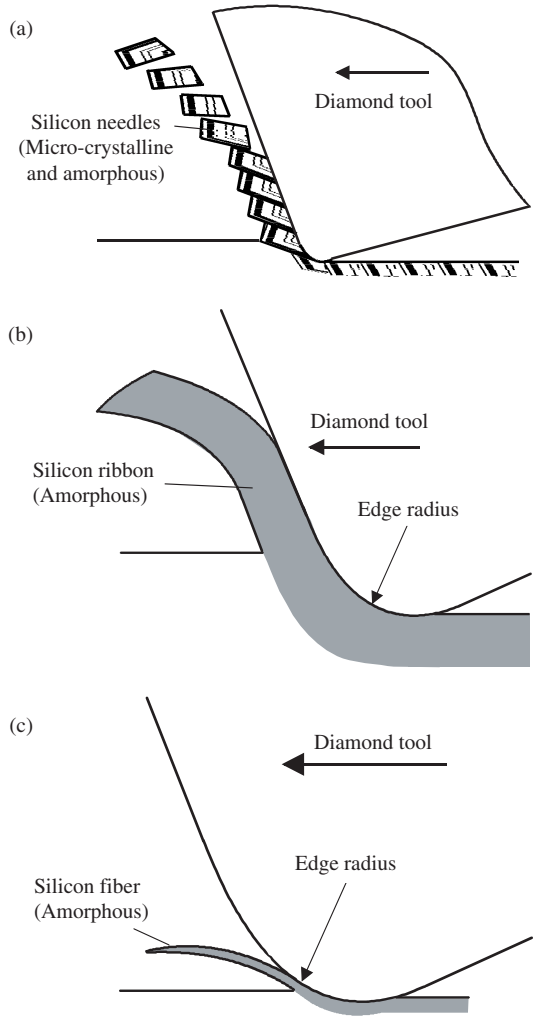

Fig. 8. Schematic models of formation mechanisms for (a) needle-type chips, (b) ribbon-type chips and (c) fiber-type chips in diamond turning of silicon.

The possible mechanism of fiber-type chip formation is presented in Figure 8(c). When the undeformed chip thickness is far smaller than the edge radius, the effective rake angle becomes excessively negative and the material is squeezed and extruded out as extremely thin amorphous chips. However, because the cutting edge profile is uneven at the nanometer level, chip formation behavior will differ from point to point along the cutting edge. This effect will give rise to segregation of the chip into fine fibers. Especially after the tool has been worn, the edge profile will be further roughened and grooved, leading to irregular fiber chips.[25] From this aspect, we can presume that by intentionally fabricating extremely fine saw-toothed grooves onto the diamond tool edge using focused ion beam (FIB) or other techniques, very long amorphous silicon nano fibers can be generated in a controllable manner.

The present work has demonstrated that it is possible to fabricate nano needles, ribbons and fibers of silicon by diamond turning. The shape and size of the chips can be changed by controlling the tool geometry and machining conditions. The microstructure of the chips is also controllable through varying the machining pressure in the machining region. Additionally, since the machining-induced amorphous silicon has higher plasticity than crystalline silicon,[26] nano ribbons and fibers produced by diamond turning may be able to improve the mechanical flexibility and electrical properties of the micro sensors and probes in nanotechnology applications. This method may also be extended to other semiconductor materials such as germanium[27] and so on, although the handling and the alignment of the nano needles, fibers and ribbons is still an issue to be investigated in the future.

4. CONCLUSIONS

Diamond turning tests were carried out on single crystal silicon and microscopic chip formation behavior was investigated. The shapes of the chips change from nano needles to nano ribbons and finally to nano fibers as the undeformed chip thickness decreases from submicron level to the nanometer level. Electron diffraction analysis showed that the needle-type chips were primarily crystalline with partial amorphization; while the ribbon-type and fiber-type silicon chips were mostly amorphous. To improve the stability and productivity of the proposed method, it is important to optimize the cutting edge geometry such as fabricating fine grooves on to the tool.

Acknowledgments: This work has been partially supported by the Japan New Energy and Industrial Technology Development Organization (NEDO).

References and Notes

1. J. Yan, K. Syoji, and T. Kuriyagawa, *J. Jpn. Soc. Prec. Eng.* 65, 1008 (**1999**).
2. J. Yan, K. Syoji, T. Kuriyagawa, and H. Suzuki, *J. Mater. Proc. Tech.* 121, 363 (**2002**).
3. J. Yan, K. Maekawa, J. Tamaki, and T. Kuriyagawa, *J. Micromech. Microeng.* 15, 1925 (**2005**).
4. S. Mack, M. A. Meitl, A. J. Baca, Z.-T. Zhu, and J. A. Rogers, *Appl. Phys. Lett.* 88, 213101 (**2006**).
5. Y. Cui and C. M. Lieber, *Science* 291, 851 (**2001**).
6. Y. Cui, Q. Q. Wei, H. Park, and C. M. Lieber, *Science* 293, 1289 (**2001**).
7. X. F. Duan, Y. Huang, Y. Cui, J. F. Wang, and C. M. Lieber, *Nature* 409, 66 (**2001**).
8. Y. Cui, Z. Zhong, D. Wang, W. U. Wang, and C. M. Lieber, *Nano Lett.* 3, 149 (**2003**).
9. W. W. Chen, H. Yao, C. H. Tzang, J. J. Zhu, M. S. Yang, and S. T. Lee, *Appl. Phys. Lett.* 88, 213104 (**2006**).
10. S. M. Prokes and S. Arnold, *Proc. SPIE* 5593, 88 (**2004**).
11. Z.-T. Zhu, E. Menard, K. Hurley, R. G. Nuzzo, and J. A. Rogers, *Appl. Phys. Lett.* 86, 133507 (**2005**).
12. Y. Sun, S. Kim, I. Adesida, and J. A. Rogers, *Appl. Phys. Lett.* 87, 083501 (**2005**).
13. K. J. Lee, M. J. Motala, M. A. Meitl, W. R. Childs, E. Menard, A. K. Shim, J. A. Rogers, and R. G. Nuzzo, *Adv. Mater.* 17, 2332 (**2005**).
14. M. A. Meitl, Z.-T. Zhu, V. Kumar, K. J. Lee, X. Feng, Y. Y. Huang, I. Adesida, R. G. Nuzzo, and J. A. Rogers, *Nat. Mater.* 5, 33 (**2006**).
15. D. Y. Khang, H. Jiang, Y. Huang, and J. A. Rogers, *Science* 311, 208 (**2006**).
16. S. R. Forrest, *Nature* 428, 911 (**2004**).
17. J. A. Rogers, K. E. Paul, R. J. Jackman, and G. M. Whitesides, *Appl. Phys. Lett.* 70, 2658 (**1997**).
18. M. Kanechika, N. Sugimoto, and Y. Mitsushima, *J. Vac. Sci. Technol. B* 20, 1298 (**2002**).
19. P. N. Blake and R. O. Scattergood, *J. Amer. Ceram. Soc.* 73, 949 (**1990**).
20. T. Nakasuji, S. Kodera, S. Hara, H. Matsunaga, N. Ikawa, and S. Shimada, *Ann. CIRP* 39, 89 (**1990**).
21. J. Yan, M. Yoshino, T. Kuriyagawa, T. Shirakashi, K. Syoji, and R. Komanduri, *Mater. Sci. Eng. A* 297, 230 (**2001**).
22. D. R. Clarke, M. C. Kroll, P. D. Kirchner, and R. F. Cook, *Phys. Rev. Lett.* 60, 2156 (**1988**).
23. G. M. Pharr, W. C. Oliver, and D. S. Harding, *J. Mater. Res.* 6, 1129 (**1991**).
24. D. L. Callahan and J. C. Morris, *J. Mater. Res.* 7, 1614 (**1992**).
25. J. Yan, K. Syoji, and J. Tamaki, *Wear* 255, 1380 (**2003**).
26. J. Yan, H. Takahashi, J. Tamaki, X. Gai, H. Harada, and J. Patten, *Appl. Phys. Lett.* 86, 181913 (**2005**).
27. J. Yan, K. Maekawa, J. Tamaki, and A. Kubo, *JSME Int. J. C* 47, 29 (**2004**).

Received: 7 June 2007. Accepted: 28 November 2007.